An EPR Investigation of Cr^{3+} and Ni^{2+} in Synthetic Pyrite Crystals

D. Siebert and R. Miller

Institut für Physikalische Chemie, Universität Freiburg i. Br.

S. Fiechter, P. Dulski, and A. Hartmann

Hahn-Meitner-Institut Berlin, Abteilung Materialforschung

Z. Naturforsch. **45a**, 1267–1272 (1990); received August 4, 1990

In many synthetic pyrite single crystals of high quality and purity we could detect Cr^{3+} and Ni^{2+} by EPR at 78 K as unwanted impurities. The assignment was possible by means of the isotopes Cr^{53} and Ni^{61}, occurring in natural abundance. The paramagnetic centers exhibit unusual g-values. In case of Ni^{2+} a ligand hyperfine interaction could be observed beside the normal hyperfine interaction with the Ni^{61} nucleus. For some crystals the Cr^{3+} signal intensity could be increased up to ten times by temperature increasement from 78 K to about 100 K. At 78 K the Cr^{3+} intensity was quenched by IR irradiation.

Key words: Pyrite, EPR, Paramagnetic ions, Conductivity.

1. Introduction

Mostly, EPR investigation is not possible in natural pyrite due to the high impurity conductivity. For synthetic crystals a lower conductivity may be obtained and often EPR measurements become possible, at least at 78 K. But even for the synthetic material the conductivity is by no means intrinsic but determined by impurities. This has to be considered in connection with the gap of about 1 eV [1]. For many photoactive applications there is a great interest in very pure material of high resistance. Therefore it is desirable to know the impurities and their nature. If they are paramagnetic, EPR offers a powerful method to investigate these centers.

In a former paper [2] we described several paramagnetic centers in synthetic crystals. These centers were either produced by the growth methods or by extra doping. Now we report of two paramagnetic centers due to Cr and Ni that were found in nearly all investigated synthetic crystals without being incorporated artificially. These centers may be related to the small paramagnetism measured by many authors [3, 4].

Reprint requests to Prof. Dr. D. Siebert, Institut für Physikalische Chemie, Albertstr. 21, D-7800 Freiburg i. Br.

2. Experimental

Details of the experimental equipment are described in [2]. The measurements were performed with an X-band spectrometer generally at 78 K. Most informations could be obtained for special orientations of the magnetic field, i.e. parallel to ⟨100⟩, ⟨110⟩, and ⟨111⟩. As the magnetic fields at resonance turned out to be very strongly orientation dependent, the crystals could be aligned wih high precision (within 0.1 degree of angle) by the site splitting patterns for the mentioned special orientations. The crystals were grown by a gas transport reaction using Br as transport agent or obtained from a Te melt [5, 6]. Stoichiometry and trace element concentrations in the crystals were measured by ICP-MS (Inductively Coupled Plasma-Mass Spectrometry). Sample preparation and operating conditions for the ICP system are given in [7].

3. EPR Results

The signals turned out to belong to two different axial centers with the local axes parallel to the four space diagonals of the cubic unit $P2_1/a\bar{3}$. In Fig. 1 a typical EPR spectrum is shown for the magnetic field H_0 parallel to ⟨110⟩. Two kinds of signals can be made out, one with a distinct hyperfine structure corre-

0932-0784 / 90 / 1100-1267 $ 01.30/0. – Please order a reprint rather than making your own copy.

sponding to a nuclear spin of 3/2, the other with a more complicated structure. The former signals could be saturated at 78 K and quenched by IR irradiation, the latter not. Therefore the signals could be distinguished even for orientations of the magnetic field, where the hyperfine structure was not resolved. In Fig. 2 the structure of the middle signal of Fig. 1 is shown in a larger scale.

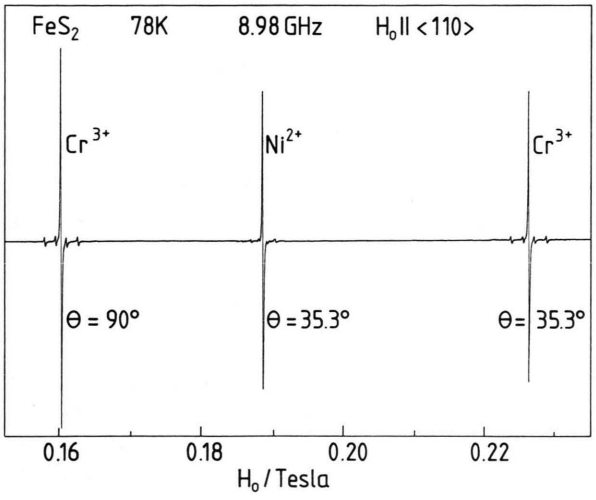

Fig. 1. EPR resonances of Cr^{3+} and Ni^{2+} at 78 K for $H_0 \parallel \langle 110 \rangle$.

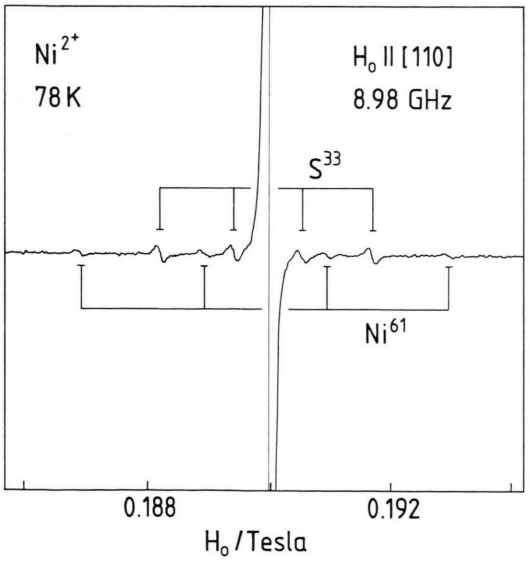

Fig. 2. Hyperfine and ligand hyperfine structure of Ni^{2+} for $H_0 \parallel \langle 110 \rangle$.

Both centers could be analyzed with the following Hamiltonian, specialized for a nuclear spin of $I = 3/2$, and an appropriate electronic spin S:

$$\mathcal{H} = g_{\parallel}\,\beta H_z S_z + (1/2)\, g_{\perp}\beta(H_+ S_- + H_- S_+) + (b_2^0/3)(3S_z^2 - S(S+1)) + A_{\parallel}\, S_z I_z + (1/2)\, A_{\perp}(S_+ I_- + S_- I_+)\,.$$

As the electronic spins turned out to be 3/2 and 1, respectively, no spin operators of higher order were necessary. For the strong central line the nuclear spin is zero and the operator of the hyperfine structure (HFS) has to be omitted. Then, only three EPR parameters have to be determined, $g_{\parallel}$, $g_{\perp}$, and b_2^0. Now, with these parameters, the Hamiltonian including the HFS operator can be used to describe the week HFS lines, and the HFS parameters can be obtained. The matrix representation of the Hamiltonian within the electronic states $|M\rangle$ for the strong lines, and within the complete states $|M, m\rangle$ for the HFS lines is straightforward and may be found in [8] for $(Cr^{53})^{3+}$ with $S = 3/2$ and $I = 3/2$. These matrices could be diagonalized numerically and resonance fields calculated together with transition probabilities. By a subsequent fitting procedure the EPR parameters could be obtained as summarized in Table 1.

3.1. Cr^{3+} on Cation Site

The resonance fields of one line of the photoactive signals varied from about 0.32 Tesla for $H_0 \parallel z$ to 0.16 Tesla for $H_0 \perp z$. This is typical for a center with $S = 3/2$ in a strong axial field. Then, further signals at rather high magnetic fields are to be expected, and indeed, we were able to observe a transition for $H_0 \perp z$ near 0.84 Tesla. This signal was too broad for detecting any hyperfine structure, but could assigned to the low field signal because of its properties of quenching and saturation. For $H_0 \parallel z$ the operator for the strong lines without hyperfine interaction is diagonal, and

Table 1. EPR parameters for Cr^{3+} and Ni^{2+} in pyrite; b_2^0 in cm^{-1}, $A_{\parallel}$, $A_{\perp}$ in 10^{-4} cm^{-1}, sign of b_2^0 from [9]; values of the last line according to Chandler et al. [9].

	$g_{\parallel}$	$g_{\perp}$	b_2^0	$A_{\parallel}$	$A_{\perp}$
Cr^{3+}	2.0163(5)	2.0095(5)	0.595(1)	12.5(1)	13.3(5)
Ni^{2+}	2.0921(5)	2.0893(5)	(−)1.208(1)	15.5(5)	13.0(5)
Ni^{2+}	2.130(5)	2.110(5)	−1.21	–	–

there is a transition between the spin states $|-1/2\rangle$ and $|1/2\rangle$ at $h\nu = g_{\parallel}\beta H_0$. From this, an exact value for $g_{\parallel}$ was obtained. The two parameters $g_{\perp}$ and b_2^0 were fitted to the two resonances for $H_0 \perp z$. Energy levels with observed transitions are plotted in Fig. 3; the agreement between measured and calculated resonance fields can be seen in Figure 4. The HFS parameters $A_{\perp}$ and $A_{\parallel}$ were obtained from the resonances at $H_0 \perp z$ and $H_0 \parallel z$, correspondingly. The intensity of the four hyperfine satellites corresponds to the natural abundance of 9.5% for Cr^{53} with nuclear spin of 3/2. As the electron spin amounts also to 3/2, we assigned the photoactive signals to Cr^{3+} on axial site. There are only two possibilities for these sites in pyrite, the cation site and the site of the anion $(S_2)^{2-}$ dumb-bells. According to the chemical nature of Cr^{3+}, its site was decided as cation site.

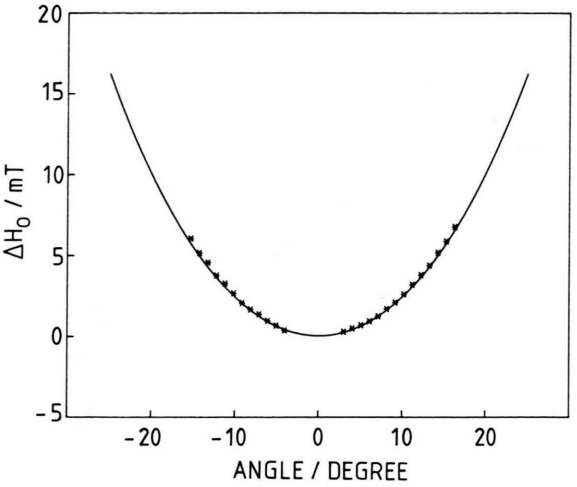

Fig. 5. Resonances near $H_0 \parallel z$ to obtain $g_{\parallel}$ for Ni^{2+}.

3.2. *Ni^{2+} on Cation Site*

One line of the non-photoactive signals decreased in intensity from a high value for $H_0 \perp z$ at 0.69 Tesla to zero for $H_0 \parallel z$ near 0.15 Tesla. This is characteristic for a transition that becomes forbidden between the pure states $|-1\rangle$ and $|1\rangle$, i.e. the spin has to be integer. The resonance field for this hypothetical transition was obtained through graphical interpolation of observed resonances near $H_0 \parallel z$ (Figure 5). From this value an exact $g_{\parallel}$ resulted from $h\nu = 2g_{\parallel}\beta H_0$. For $H_0 \parallel z$ another very strong resonance could be observed near 0.94 Tesla. On the assumption that the electronic spin is $S=1$, the EPR parameter b_2^0 followed from the diagonal representation of the Spin Hamiltonian (energy diagram in Figure 6). Now the transition for $H_0 \perp z$ could be easily fitted by an appropriate value for $g_{\perp}$. With these EPR-parameters all the other transitions for the different orientations could be obtained in excellent agreement with the experimental values (see Figure 7). By this the spin value $S=1$ is proved. From Fig. 2, two quartets of very low intensity can be distinguished, corresponding to an interaction with a nuclear spin of $I=3/2$. As these quartets could not be observed for $H_0 \parallel z$ and $H_0 \perp z$ the corresponding EPR parameters had to be fitted for intermediate directions. This is demonstrated in Fig. 8 for the weaker quartet. The anisotropy of the splitting is mainly not due to the small anisotropy of the HFS parameters but due to the large b_2^0 that determines the strong axial character of the center. The intensity of this quartet with the greater splitting is in agreement with a natural abundance of about 1%. Therefore we assign the paramagnetic center to Ni^{2+} on cation site, the natural abundance of Ni^{61} with nuclear spin $I=3/2$ being 1.13%. The other quartet of higher intensity and lower splitting was associated with the interaction of one sulfur ligand isotope S^{33}, nuclear spin being 3/2 and natural abundance 0.75%. The probability that one of the six ligands surrounding the Ni center will be a S^{33} isotope amounts to 3.7%. The probability that two or more ligands will have a nuclear spin all at once is vanishingly small. This corresponds to the observed intensity if one assumes that the influence of the ligands is the same for all the six crystallographically equivalent ligands. The ligand hyperfine interaction could be analyzed by the same Hamiltonian as before, now with $A_{\parallel} = A_{\perp} = A_0 = 0.0009\ cm^{-1}$. The anisotropy of the splitting is similar as in Fig. 8 and again a consequence of the large b_2^0. The isotropy A_0 means that also the interaction with a single ligand is mainly isotrop and expressed by the same value, its anisotropy being too small to be detected.

EPR of Ni^{2+} that was incorporated artificially in pyrite, was also observed by Chandler et al. [9], but without any hyperfine structure (Table 1).

4. Discussion

Typical values for the impurity concentration of the crystals from the Te melt are about 10 μg/g for Cr and

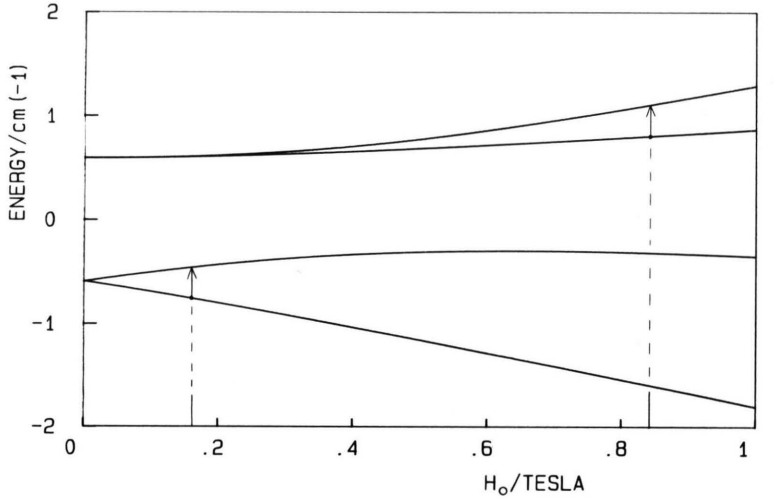

Fig. 3. Energy diagram for Cr^{3+} for $H_0 \perp z$ with observed transitions.

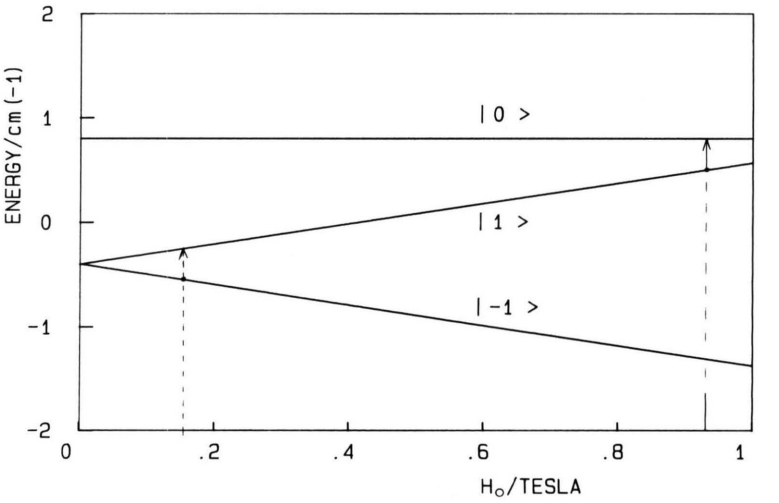

Fig. 6. Energy diagram for Ni^{2+} for $H_0 \parallel z$ with extrapolated and observed transition.

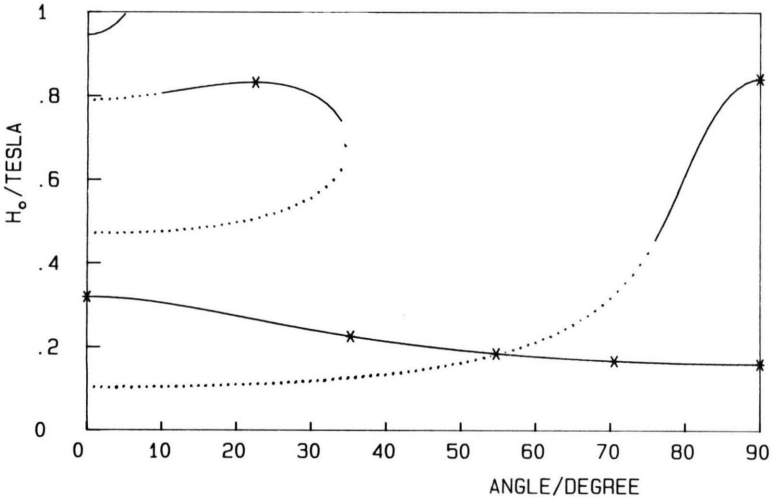

Fig. 4. Angular dependence of the resonance fields H_0 for Cr^{3+};
———, · · · · · calculated values, * * * experimental values;
· · · · · small transition probability.

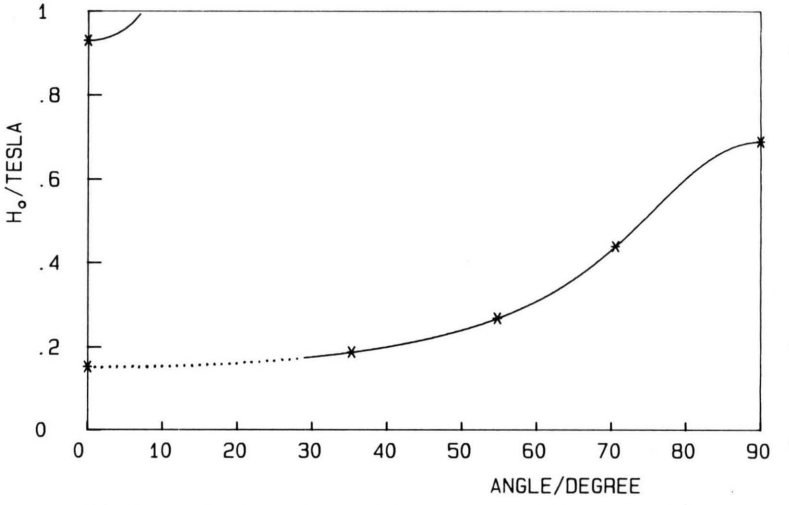

Fig. 7. Angular dependence of the resonance fields H_0 for Ni^{2+};
———, · · · · · calculated values, * * * experimental values;
· · · · · small transition probability.

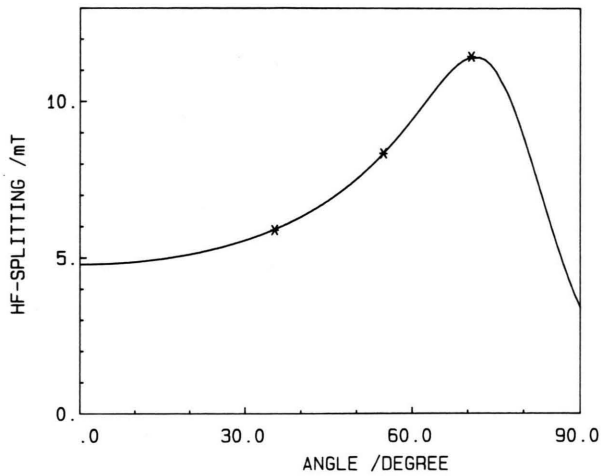

Fig. 8. Angular dependence of the HF splitting for Ni^{2+}; —— calculated splitting, * * * experimental values.

20 μg/g for Ni, obtained by ICP measurements. The limiting values by this method were 0.5 μg/g and 1 μg/g, respectively. As the corresponding EPR signals could be observed very well, the sensitivity of the detection by EPR turned out to be better by a factor of about 20 for some of the investigated crystals. It is worth mentioning that neither in the solvent Te nor in the elements used for pyrite synthesis a trace element concentration of Cr and Ni of this order of magnitude was detectable. For this reason it has to be concluded that the pyrite structure favours the enrichment of both elements during crystallization. This fact can be explained by the high crystal field stabilization energies of Ni and Cr in a strong octahedral ligand field, its strength being well documented by the low-spin states Fe^{2+} and Mn^{2+} in pyrite [2]. NiS_2 itself crystallizes in the pyrite structure and is a well known Mott insulator [10]. But there is no CrS_2 crystallizing in this structure, and only in $CrSb_2$, which crystallizes in the pyrite related marcasite structure, chromium exhibits an octahedral anion coordination [11]. In nature, both elements are mainly responsible for the material's paramagnetism at temperatures below 100 K [3]. The total amount of the trace elements in synthetic crystals could also be quantified from magnetic susceptibility measurements, which fitted very well to those trace elements amounts found by ICP measurements [4].

4.1. EPR Parameter

The most striking result is the great g-value for Cr^{3+}, greater than the free electron value. This contradicts the common rule that for ions with d electron shell less than half full the g-shift should be negative. As this rule results from a pure crystal-field model, we conclude that in pyrite strong covalent bonding exists. This will be supported by results obtained from far-infrared reflection spectra [12]. Nevertheless it is worthwhile to note that for all about one hundred EPR examples of Cr^{3+} listed in [13] there is none with such a positive g-shift. The A-values in pyrite are significantly smaller than in octahedral environment of oxygen and even smaller than in MgS, where A amounts to $15.3 \times 10^{-4}\,cm^{-1}$ [14]. This may also be explained by the greater covalency of the sulphur bond in pyrite that removes the electrons from the nucleus.

The g-values of Ni^{2+} in pyrite are greater than the free electron value, as it should be for more than five d-electrons, but smaller than usually (2.20–2.25 in many oxides). The discrepancy with the value of Chandler et al. [9] may be explained by the fact that these authors could not investigate the transition $|-1\rangle - |1\rangle$ near $H_0 \parallel z$, because their resonances were not so intense and they used Q-band frequencies, for which these transitions are more forbidden. – A-values for Ni^{2+} are very rare in the literature according to the small natural abundance of 1.1% for the Ni^{61} isotope.

4.2. Impurity Conductivity

If an impurity center influences the conductivity by furnishing electrons or holes, a change of its charge state must occur, i.e. at least one of the charge states will be paramagnetic and observable by EPR, in principle. The impurity center will be of special importance if this change of its charge state occurs at temperatures for which the conductivity is of interest.

There are several reasons indicating that the Ni impurity does not determine the conductivity directly. Ni^{2+} is isovalent to Fe^{2+}, and no change of charge state was observed, neither by temperature variation nor by IR irradiation. Furthermore it seems to be possible to obtain $Ni_xFe_{1-x}S_2$ up to $x<0.1$ [9].

The situation for the incorporation of Cr is quite different. We detect Cr^{3+}, so there will be a tendency to pick up one electron. In fact we observed for many crystals an increase of the Cr^{3+} signal intensity accompanied by an increase of the conductivity by raising the temperature from 78 K upwards. We assume therefore that Cr^{2+} acts as a donor for electrons, Cr^{3+}

being the ionized donor, visible by EPR, while Cr^{2+} is not visible in our experiments. But surely that is not the only mechanism for the conductivity of our crystals, for by raising the temperature furthermore, the Cr^{3+} signal intensity decreased, whereas the conductivity increased monotonically, indicating another mechanism for conductivity. At 78 K IR radiation quenched the Cr^{3+} signal abruptly, the conductivity increased. After the irradiation the conductivity dropped immediately to its low value at 78 K, but the Cr^{3+} signal recovered only within hours. This may be explained by other impurity levels above the valence band that become ionized by the IR radiation whereby the produced electrons will discharge Cr^{3+} to Cr^{2+}. Further investigations are necessary to clarify the complex situation.

Acknowledgements

Financial support of this work by the "Fonds der Chemischen Industrie" is gratefully acknowledged.

[1] A. Ennaoui, S. Fiechter, W. Jaegemann, and H. Tributsch, J. Electrochem. Soc. **133,** 97 (1986).
[2] D. Siebert, J. Dahlem, S. Fiechter, and A. Hartmann, Z. Naturforsch. **44a,** 59 (1989).
[3] P. Burgardt and M. S. Seehra, Solid State Comm. **22,** 153 (1977).
[4] W. Müller, H. H. Bertschat, K. Biedermann, R. Kowallik, E. Lahmer-Naim, H.-E- Mahnke, S. Seeger, W.-D. Zeitz, S. Fiechter, and H. Tributsch, Phys. Rev. **B 41,** 8624 (1990).
[5] S. Fiechter, J. Mai, A. Ennaoui, and W. Szacki, J. Crystal Growth **78,** 438 (1986).
[6] J. G. Fleming, J. Crystal Growth **92,** 287 (1988).
[7] J. Luck, A. Hartmann, and S. Fiechter, Fresenius Z. Anal. Chem. **334,** 441 (1989).
[8] W. Low, Paramagnetic Resonance in Solids, in: Solid State Physics, Supplement 2, p. 51, Academic Press 1960.
[9] R. N. Chandler and R. W. Bené, Phys. Rev. **B 8,** 4979 (1973).
[10] S. Ogawa, J. Appl. Phys. **50,** 2308 (1979).
[11] G. Brostigen and A. Kjekshus, Acta Chemica Scandinavia **24,** 2993 (1970).
[12] H. D. Lutz, G. Kliche, and H. Haeuseler, Z. Naturforsch. **36a,** 184 (1981).
[13] S. A. Al'tshuler and B. M. Kozyrev, Electron Paramagnetic Resonance in Compounds of Transition Elements, John Wiley & Sons, New York 1974.
[14] P. Auzins, J. W. Orton, and J. E. Wertz, Proc. 1st Int. Conf. I, 90 (1963).